Available online at www.sciencedirect.com
SCIENCE DIRECT®
Journal of Magnetic Resonance 163 (2003) 1–7
JMR Journal of Magnetic Resonance
www.elsevier.com/locate/jmr

Single point measurements of magnetic field gradient waveform

David J. Goodyear,[a] Maurice Shea,[a] Steven D. Beyea,[a] Nadim J. Shah,[b] and Bruce J. Balcom[a,*]

[a] *MRI Centre, Department of Physics, P.O. Box 4400, University of New Brunswick, Fredericton, New Brunswick, Canada E3B 5A3*
[b] *Institut fuer Medizen, Forschungszentrum, Juelich 52428, Germany*

Received 3 September 2002; revised 25 April 2003

Abstract

Pulsed magnetic field gradients are fundamental to spatial encoding and diffusion weighting in magnetic resonance. The ideal pulsed magnetic field gradient should have negligible rise and fall times, however, there are physical limits to how fast the magnetic field gradient may change with time. Finite gradient switching times, and transient, secondary, induced magnetic field gradients (eddy currents) alter the ideal gradient waveform and may introduce a variety of undesirable image artifacts. We have developed a new method to measure the complete magnetic field gradient waveform. The measurement employs a heavily doped test sample with short MR relaxation times (T_1, T_2, and $T_2^* < 100$ μs) and a series of closely spaced broadband radiofrequency excitations, combined with single point data acquisition. This technique, a measure of evolving signal phase, directly determines the magnetic field gradient waveform experienced by the test sample. The measurement is sensitive to low level transient magnetic fields produced by eddy currents and other short and long time constant non-ideal gradient waveform behaviors. Data analysis is particularly facile permitting a very ready experimental check of gradient performance.

Keywords: Gradient; Waveform; Single point; **k**-Space; Eddy current

1. Introduction

Pulsed magnetic field gradients are fundamental to spatial encoding and diffusion weighting in magnetic resonance and magnetic resonance imaging. Non-ideal magnetic field gradient pulses have finite rise and decay times with unwanted transient, eddy current related, magnetic field gradients contributing to and often dominating the ideal behavior [1]. These secondary transient magnetic field gradients result from gradient switch induced eddy currents in the cold conductive material of the magnet superstructure, and other surrounding materials. Non-ideal gradient waveforms lead to intensity artifacts in MRI images and phase/baseline artifacts in spectra obtained using localized spectroscopy techniques [2]. If the magnetic field gradient waveform experienced by the sample is known, then the waveform can be adjusted or compensated to closer approximate ideal behavior. Alternatively, knowledge of the true gradient waveform may be used in data post-processing to minimize image artifacts and spectral distortions [3–6]. The on-going drive for more rapid and higher resolution MRI means that precise, accurately switched, magnetic field gradients are of increasing contemporary importance.

Numerous methods for measuring eddy current effects and magnetic field gradient waveforms have been presented in the literature. One common method for acquiring a magnetic field gradient waveform involves measuring the induced voltage in a flux coil [7]. This particular method is sensitive to magnetic fields changing rapidly in time but is somewhat insensitive to slowly varying transient fields. Methods described by Wysong et al. [8] and Boesch et al. [9] exploit the off-resonance behavior of the NMR signal in the presence of transient magnetic fields to set compensation networks [10,11]. These methods provide information about the off resonance behavior of the free induction decay (FID) resulting from the time evolution of transient fields

* Corresponding author. Fax: +506-453-4581.
E-mail address: bjb@unb.ca (B.J. Balcom).

1090-7807/03/$ - see front matter © 2003 Elsevier Science (USA). All rights reserved.
doi:10.1016/S1090-7807(03)00152-6

following a magnetic field gradient pulse. Increased interest in diffusion-weighted EPI has led to several new methods, for measuring and setting gradient pre-emphasis networks [12]. However, none of these techniques [8–12] provide direct information about the shape of the full magnetic field gradient waveform.

Magnetic field gradient pulse shapes have been determined using NMR techniques proposed by Takahashi et al. [7] and Yamamoto et al. [3]. The first uses a self encoding field gradient which calibrates the gradient shape to be measured and the results are obtained in the form of a time integral of the gradient pulse. The second technique utilizes NMR signals acquired from a uniform sample, in the presence of a gradient pulse, to calculate the gradient amplitude at a given time in terms of the ratio of the FID and its derivative. An additional method proposed by Lee et al. [13] involves calculating the time derivative of the acquired NMR signal phase, which is proportional to the amplitude of the gradient pulse, at a given time point. More recent measurements of the evolving signal phase during magnetic field gradient waveforms have become quite sophisticated [14]. Such measurements are of critical importance for regridding algorithms in spiral scan MRI.

The method presented is a logical, yet quite general, development of the single point profile method presented by Balcom et al. [1]. Our earlier work required the repetitive application of a complete series of phase encode gradients leading to the reconstruction of a simple phantom image. Contraction of the phantom image, through the similarity theorem of fourier transforms, then permitted one to assign a relative gradient attenuation which would be assumed to be true for all phase encode gradient steps. The current technique is a reciprocal space method which permits one to more directly examine the phase behavior of arbitrarily complicated single gradient waveforms.

The technique employs a uniform test sample with short relaxation times (T_1, T_2, and $T_2^* < 100$ μs) and a series of closely spaced radiofrequency excitations, combined with single point data acquisitions. This technique measures evolving signal phase in the presence of a magnetic field gradient pulse and directly determines the magnetic field gradient waveform experienced by the sample. The measurement is sensitive to low amplitude transient magnetic fields produced by eddy currents and other non-ideal gradient waveform behaviors. One of the appealing characteristics of the method is that it is not probe specific. The possibility for this method to be used as a diagnostic tool for pre-emphasis settings, and for classifying non-ideal gradient behaviors due to the presence of NMR probes and other conductive media, is presented.

Many methods have been proposed to measure arbitrary **k**-space trajectories [7,14]. We anticipate this method may also be used to determine **k**-space trajectories for use in **k**-space re-gridding and image reconstruction. The principal advantages of the method are its experimental and data processing simplicity. The main source of uncertainty is the experimental uncertainty of the signal phase, which increases at low experimental signal to noise ratios.

2. Theory

We assume radiofrequency (RF) excitation of a uniform test sample with a broadband RF pulse. Following the RF pulse, the FID phase evolves for a time t_p, which we term the encoding time. Short T_2^* lifetimes reduce the signal amplitude during time t_p, but do not alter the signal phase. The single point magnetic resonance signal of a three-dimensional object in the presence of a spatially and time varying magnetic field gradient $G_z(t)$ at time t_p after the RF excitation pulse is

$$S(t_p) = \int_{-\infty}^{\infty}\int_{-\infty}^{\infty}\int_{-\infty}^{\infty} \rho(x,y,z) e^{i\theta(z,t_p)}\,dx\,dy\,dz, \tag{1}$$

where ρ(x,y,z) is the spin density.

The accumulated signal phase, of isochromats with position z and gyromagnetic ratio γ, is given by Eq. (2).

$$\theta(z,t_p) = \gamma \int_0^{t_p} G_z(t) z\,dt. \tag{2}$$

If a cylinder with uniform spin density is oriented lengthwise along the magnetic field gradient axis the cross-sectional area is constant over the length of the object. This is analogous to a one-dimensional sample with a uniform proton spin density $\rho(z)$ oriented lengthwise along the magnetic field gradient axis as shown in Fig. 1. It is possible to work with other phantom geometries, for example spherical, however in this case the proton density weighting is no longer uniform, and the resulting equations become more difficult to work with and the simple intuitive interpretation of the results is lost.

Assuming a uniform cylindrical phantom geometry, Eq. (1) may be written as

$$S(t_p) = \int_a^b \cos\left[\theta(z,t_p)\right] + i\sin\left[\theta(z,t_p)\right] dz, \tag{3}$$

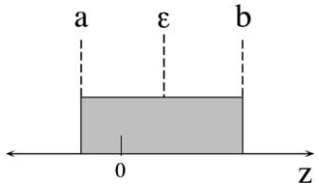

Fig. 1. One-dimensional spin density $\rho(z)$ of a uniform cylindrical sample oriented parallel to the axis of a magnetic field gradient. Coordinates a and b define the ends of the sample while ε defines the center of the sample relative to the coordinate origin.

where a and b define the left and right ends of the cylinder with $\rho(z)$ set equal to unity.

In order to extract the magnetic field gradient amplitude from the experimental signal, Eq. (2) may be further simplified using the mean value theorem for integrals. The magnetic field gradient pulse interacting with the sample is a continuous function of time on the interval $[0, t_p]$. There exists a time t' on the interval $(0, t_p)$ such that

$$\int_0^{t_p} G_z(t)\,dt = G_z(t')t_p \tag{4}$$

or similarly, $G_z(t')$ is the mean value of $G_z(t)$ during the encoding time interval. If we choose an encoding time which is short compared to the characteristic rise and decay of the magnetic field gradient pulse, then it is reasonable to assume that the gradient amplitude changes linearly during the encoding time. This allows us to assign a unique time point to the gradient amplitude measurement. For a linearly varying gradient, the assigned time point, t', is simply the midpoint of the interval or $t_p/2$. The equivalence of the gradient areas defined by the integral in Eq. (4) and the product $G_z(t')\,t_p$, which is depicted in Fig. 2, allows one to simplify Eq. (2)

$$\theta(z, t_p) = \gamma G_z(t')t_p z. \tag{5}$$

Incorporating Eq. (5), and integrating over the length of the cylindrical sample, the single point NMR signal given in Eq. (3) yields

$$S(t_p) = \frac{\left[\sin\left(\gamma G_z(t')t_p b\right) - \sin\left(\gamma G_z(t')t_p a\right)\right] + i\left[\cos\left(\gamma G_z(t')t_p a\right) - \cos\left(\gamma G_z(t')t_p b\right)\right]}{\gamma G_z(t')t_p}. \tag{6}$$

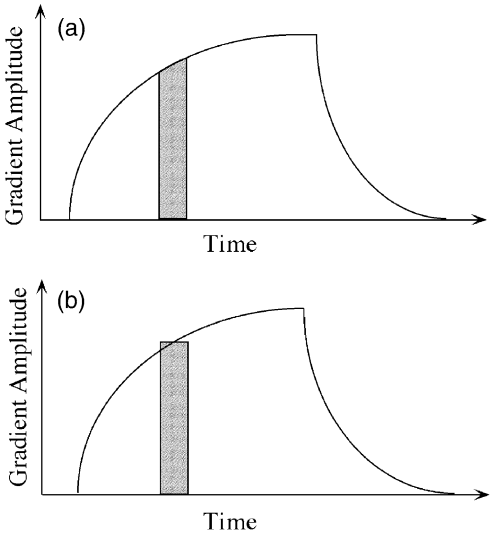

Fig. 2. The technique measures signal phase during a short duration t_p (encoding time) after an RF pulse is applied to the uniform sample. The gradient waveform is grossly non-ideal for ease of illustration. (a) At the end of the encoding time the signal phase is proportional to the gradient area (shaded region) on an interval defined by the encoding time t_p. (b) If the encoding time is short compared to the characteristic rise or decay time of the gradient pulse, then the gradient changes linearly during t_p. The gradient area in (a) may then be equated to the area $G(t')t_p$, where $G(t')$ represents the gradient amplitude at the midpoint of the encoding time interval.

The observed signal is inversely proportional to the average gradient amplitude during the encoding time. For large gradient amplitudes therefore the signal may drop to such low values that random noise will hinder an accurate phase determination. These effects may be reduced through the choice of an appropriately short phase encode time t_p.

In order to obtain $G_z(t')$ in terms of signal phase we recognize that there is a time varying phase angle between the real and imaginary components of the signal. Extracting the time-dependent phase angle from Eq. (6), and using sine double angle formulae we arrive at

$$\phi = \gamma G_z(t')t_p\left(\frac{b+a}{2}\right) = \gamma G_z(t')t_p\varepsilon, \tag{7}$$

which can be rearranged to give

$$G_z(t') = \frac{\phi}{\gamma t_p \varepsilon}, \tag{8}$$

where $\varepsilon = (b+a)/2$ is the offset of the sample center from the origin of the axis along which the spatially varying gradient is applied. This offset is illustrated in Fig. 1.

Eq. (8) shows that the signal phase is directly proportional to the instantaneous gradient amplitude, as well as the encoding time and sample offset. Increasing any one of these parameters will increase the observed phase accumulation. Since the encoding time and sample offset are fixed for a specific measurement, the signal phase is thus a direct measurement of average gradient amplitude during the chosen measurement interval. This interval may quite reasonably encompass short time periods during gradient rise, stabilization and decay in arbitrarily complicated gradient waveforms. A systematic series of such measurements will thus map out the complete magnetic field gradient waveform.

3. Experimental methods

A heavily doped 2% agar gel was prepared using a 600 mM solution of $GdCl_3$ (Aldrich, Milwaukee, WI) in a cylindrical glass tube with a diameter of 1 cm and

length of 5 cm. The phantom had a T_2^* of approximately 60 μs. With such a short value, the T_2 is assumed to be equal to T_2^*, as is the T_1. The ends of the sample were cut using a razor blade and guide to make a well-defined right cylinder. The cylinder ends were capped using teflon plugs to prevent drying. The final cylindrical sample had a length of approximately 16 mm.

Experiments were performed using commercial (Morris Instruments, Ottawa, Ont.) and homebuilt quadrature birdcage resonators. The probes were driven by a 2 kW AMT (Brea, CA) 3445 RF amplifier and experiments were carried out in a Nalorac (Martinez, CA) 2.4 T 32 cm bore superconducting magnet with a Nalorac gradient insert that was water cooled and self-shielded. The gradient set had a Nalorac pre-emphasis unit, Nalorac shim controller, and was powered by a Techron (Elkhart, IN) 8710 gradient amplifier system. The spectrometer console was a Tecmag (Houston, TX) Libra S-16. Pulse programs and data acquisition were controlled by a Macintosh Quadra 950 running MacNMR.

The pulse sequence used for the experiments is similar to the sequence presented in Fig. 3. Thirty-two broadband RF pulses were typically applied in each execution of the pulse sequence. Low flip angle pulses were used to ensure minimal perturbation of longitudinal magnetization from pulse to pulse. The spacing between RF pulses was 260 μs with each pulse lasting 10 μs, corresponding to a flip angle of 24°. Brief duration RF pulses were applied in order to ensure uniform excitation of the broad line sample.

Quadrature phase cycling was employed, and four signal averages were collected, during each experiment. Early and late RF pulses in the sequence were used to obtain a reference signal phase from which a baseline could be determined for the gradient waveform. Eleven equally spaced RF pulses were applied during the gradient rise to acquire signal phase at a series of times after the gradient had been switched on. The pulse-encode events applied to the phantom after the gradient has been switched off are used to measure evolution of signal phase in the presence of the decaying gradient up to 5 ms after the gradient switch off. Each RF pulse corresponds to a discrete measurement of gradient amplitude during the encoding time. The entire gradient waveform, at high temporal resolution, was measured by repeating the pulse sequence with the addition of small time increments, τ, as illustrated in Fig. 3. A final 5 μs per point resolution was chosen for the 32 pulse sequence, and the encoding time, t_p, was chosen to be 40 μs. Total measurement times were usually less than 3 min.

An experimental time resolution on the gradient waveform which is less than the encoding time t_p requires the application of RF pulses which are systematically shifted in time τ with repetitive application of the basic pulse sequence represented by Fig. 3. These time shifted measurements measure partially overlapping gradient areas as illustrated in Fig. 4.

When the arctangent function is used to calculate the signal phase, the phase angle plus multiples of π are indistinguishable. This was particularly important when the gradient amplitude is large enough to cause the signal vector to change quadrants during an individual pulse-encode measurement. This phase angle wrapping leads to distinct discontinuities in the gradient waveform which can be corrected simply by adding multiples of π to the signal phase where the wraps occur. Alternatively, one can choose a maximum phase for a given maximum gradient amplitude simply by choosing an appropriate t_p or sample offset ε such that wrapping will not occur. Data processing was carried out using several routines written in IDL (Research Systems, Boulder, CO).

The cylindrical sample was oriented inside the probe such that the longitudinal axis was parallel to the direction of the chosen magnetic field gradient. Before performing the gradient waveform experiments the sample offset ε was measured using one-dimensional SPRITE images [15]. The SPRITE imaging method is well suited for imaging semi-rigid polymers and other

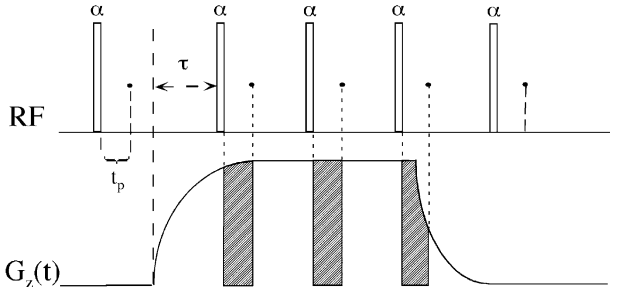

Fig. 3. Schematic of the pulse sequence used to acquire gradient waveforms. RF pulses prior to, and after, the gradient pulse establish an experimental baseline phase. The shaded area represents the product of the gradient and encoding time t_p which determines signal phase. Repetitive applications of the basic pulse sequence have time τ incremented to yield high temporal resolution in the final measurement.

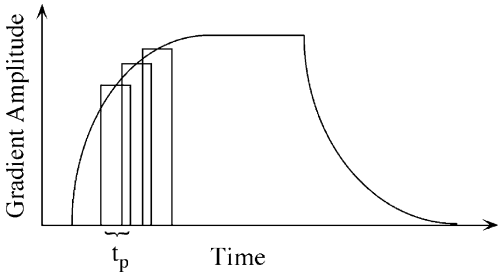

Fig. 4. When the spacing between gradient time points, in repetitive applications of the pulse sequence, is less than the encoding time, the experiment measures overlapping gradient areas with increased overall temporal resolution. The gradient waveform is grossly non-ideal for ease of illustration.

systems containing short relaxation time nuclei, such as the gel phantom used in these experiments.

4. Results and discussion

Fig. 5 shows two magnetic field gradient pulses, of opposite polarity, measured using the method described. Each gradient pulse had a nominal amplitude of ±1 G/cm and a duration of 3 ms The magnetic field gradient pulses, overlaid in the figure, were measured in separate experiments. The offset ε was measured to be 17 mm. Eq. (8) illustrates the direct relationship between signal phase and the instantaneous gradient amplitude. If the sign of the gradient is altered, this changes the sign of the signal phase. Because the signal phase and gradient amplitude are directly proportional, Eq. (8), we may plot the signal phase as gradient amplitude, assuming that the phase corresponding to the maximum gradient is known. The maximum phase is equated to the chosen gradient maximum determined at gradient stabilization. All displayed gradient amplitudes are thus scaled to an assumed gradient maximum in each experiment. There is a small but measurable difference between the absolute value of the peak gradient amplitudes for these bipolar pulses. A long duration low amplitude decay component is observed following each gradient pulse.

The method is useful for inspecting low amplitude, long decay time constant gradients which may result from incorrect pre-emphasis settings or eddy currents. Figs. 6a and b present gradient pulses with amplitudes of 2.5 G/cm, duration 3 ms, measured using sample offsets ε of 15 and 41 mm, respectively. The first 32 data points, prior to 0 ms, and the last 52 data points, after 8.0 ms, define a gradient baseline. The time interval between baseline data points is 50 ms, i.e., the measurement time interval is not the same for the gradient baseline measurement as it is for the gradient waveform measurement. The first post-gradient baseline measurement was 50 ms after switch-off to ensure complete decay of any residual gradient. The inset in Fig. 6a and b shows an expanded view of the gradient, revealing a low amplitude, long time constant, decay after gradient switch off. The insets also clearly reveal the differences between the still evolving gradient and the true baseline.

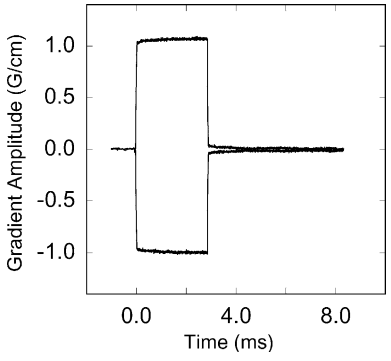

Fig. 5. Experimental magnetic field gradient waveforms, G_x, determined with the pulse sequence of Fig. 3. The nominal gradient strength was ±1 G/cm with a gradient pulse duration of 3 ms.

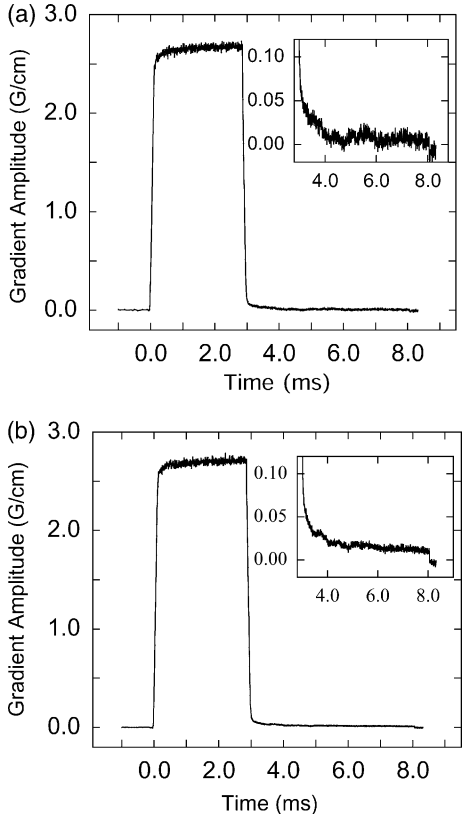

Fig. 6. Experimental measurement of the G_x gradient undertaken with the pulse sequence of Fig. 3. The pre-emphasis network settings were not optimized. The inset figures show an expanded view of the baseline revealing a low amplitude, long time constant decay after the gradient pulse has been turned off. The sample offset ε was changed from (a) to (b). Gradient baseline data points have a reduced temporal resolution, 50 ms.

The inset in Fig. 6a illustrates a low amplitude gradient decay, with substantial noise, measured with a sample offset of 15 mm. By increasing the sample offset to 41 mm, the amplitude of the low-level gradient is more accurately determined, inset Fig. 6b. This is predictable from Eq. (7) which shows that the signal phase is directly proportional to the sample offset, which permits a more precise measurement of smaller phase differences—and hence small gradient differences. Phase angle unwrapping was applied to both gradient waveforms.

The uncertainty in the maximum gradient amplitude measurement has apparently increased in Fig. 6, as compared to the gradient pulses presented in Fig. 5. The signal strength predicted by Eq. (6) is inversely proportional to the gradient amplitude during the encoding time. For increasing gradient strength, the signal

amplitude will decrease. At maximum gradient amplitude, the signal phase determination may be adversely affected by random noise. If one wishes to observe low amplitude gradients, or portions of a gradient waveform with low amplitude gradients, then this potential problem is avoided. Magnetic field gradient pre-emphasis settings may be guided by this method through examination of the low amplitude residual gradients following gradient switch off.

The sensitivity of the method to low amplitude magnetic field gradients may be estimated based on a reasonable phantom size and displacement with reasonable estimates of phase signal to noise. Our estimate of the minimum detectable gradient, of the order of 0.01 G, is in accord with the results of Fig. 6a.

The method yields a set of average gradient amplitudes during the encoding time for each pulse-encode event, recorded at sequentially later times in the waveform. It is important to note, when using a time spacing which is less then the encoding time, that each measurement of gradient amplitude will overlap subsequent measurements if gradient areas overlap as illustrated in Fig. 4. In cases where gradient pulses exhibit extremely rapid fluctuations, the running average effect of the measurement will lead to a broadening/smoothing of the waveform.

In the limit of no phase angle wrapping, with appropriate experimental limits on t_p, ε and the maximum gradient, a simple and direct display of signal phase from successive RF pulses is a robust measure of the gradient waveform. The minimum encoding time t_p is limited by the ring down time of the RF probe employed in the measurement. Spectrometers which are able to display signal phase from single point acquisitions, will directly reproduce on the spectrometer display, with no data processing, the magnetic field gradient waveform. Increasing the temporal resolution does require multiple applications of the pulse sequence, with subsequent interleaving of the experimental data prior to display.

It should be noted that this method will be sensitive to B_0 shifts which may accompany magnetic field gradient pulses. In this case the spatially constant, but temporally varying, magnetic field change will introduce phase changes which may be interpreted as gradient changes. While in principle it may be possible to differentiate these cases by altering the position of the phantom, a better and simpler solution is to use alternate methods of measuring and compensating for B_0 shifts.

The current method may be employed to measure more sophisticated magnetic field gradient waveforms. Fig. 7 presents a measurement of the gradient waveform for a set of three rapidly switched bipolar gradients. The sequence used to measure this waveform included four equally spaced RF pulses for each gradient switch. The spacing between pulses was 260 μs. The ultimate time resolution, following multiple interleaves, during the gradient waveform was 5 μs. It is important to note that the experimental measurement shows that the positive and negative gradient lobes differ in peak amplitude. In addition, the experiment shows there are waveform differences between consecutive positive, and consecutive negative, gradient lobes. Note in particular the differences in width of the first two gradient lobes. This indicates that the gradient time history alters the behavior of subsequent pulses, when eddy current effects have not reached a steady state. This would clearly be an undesirable characteristic for high speed imaging techniques where fast gradient switches are required.

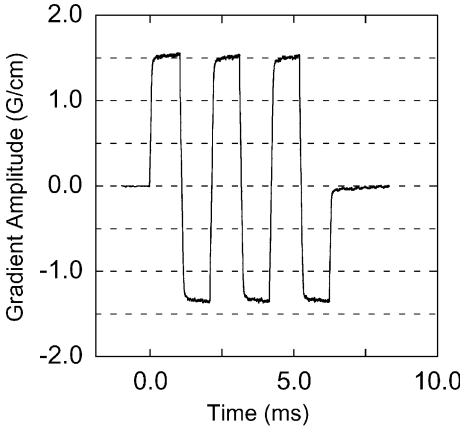

Fig. 7. Rapidly switched bipolar gradients, G_z, measured with the pulse sequence of Fig. 3. Each gradient lobe has a nominal duration of 1 ms with a nominal amplitude of ±1.5 G/cm. The experimental waveform clearly illustrates systematic non-ideal behavior in the component lobes.

Non-ideal gradient waveforms may lead to image distortions due to the deviation of the acquired **k**-space points from the expected **k**-space trajectory. Many methods have been recently proposed to determine the true **k**-space trajectories, for rapid MRI, techniques which can be used during image processing to compensate for non-ideal gradient behavior [7,14,16]. The method is sufficiently flexible, through variation of all parameters, to be generally applicable, even to whole body instruments where the gradient performance is extremely demanding. Here a predetermined gradient waveform could be used to form a 'look-up' table for use in image reconstruction schemes, particularly for EPI, which is sensitive to even small amplitude long-term eddy currents.

5. Conclusion

We have presented a single point measurement of magnetic field gradient waveforms which accurately reproduces the gradient time history of a test sample. The method yields information concerning gradient behavior during gradient rise, stabilization, and decay. This

information can be used to set pre-emphasis networks, diagnose eddy current hardware problems, or it may be used to trace **k**-space trajectories for input to image reconstruction algorithms. We have found the method of great practical use for the first two applications, and anticipate similar benefits in the third.

The measurement requires a specialized, but easily fabricated, test sample. The strongest features of the technique are its ease of implementation, its minimal data processing and ease of interpretation.

Acknowledgments

B.J.B. thanks NSERC of Canada for operating and equipment grants, as well as a Steacie Fellowship for 2000-2002. The UNB MRI Centre is supported by an NSERC Major Facilities Access award. B.J.B. is the holder of a Canada Research Chair. D.J.G. thanks NSERC of Canada for a postgraduate scholarship.

References

[1] B.J. Balcom, M. Bogdan, R.L. Armstrong, Single point imaging of gradient rise, stabilization, decay, J. Magn. Reson. A 118 (1996) 122–125.

[2] D.G. Hughes, S. Robertson, P.S. Allen, Intensity artifacts in MRI caused by gradient switching in an animal-size magnet, Magn. Reson. Med. 25 (1992) 167–179.

[3] E. Yamamoto, H. Kohno, Gradient time-shape measurement by NMR, J. Phys. E: Sci. Instrum. 19 (1986) 708–711.

[4] J. Frahm, W. Hanicke, Signal restoration for NMR imaging using time-dependent gradients, J. Phys. E: Sci. Instrum. 17 (1984) 612–616.

[5] M.M. Tropper, Image reconstruction of the NMR echo-planar technique and for a proposed adaptation to allow continuous data acquisition, J. Magn. Reson. 42 (1981) 193–202.

[6] U. Klose, In vivo proton spectroscopy in the presence of eddy currents, Magn. Reson. Med. 14 (1990) 26–30.

[7] A. Takahashi, T. Peters, Compensation of multi-dimensional selective excitation pulses using measured *k*-space trajectories, Magn. Reson. Med. 34 (1987) 446–456.

[8] R.E. Wysong, I.J. Lowe, A simple method of measuring gradient induced eddy currents to set compensation networks, Magn. Reson. Med. 29 (1993) 119–121.

[9] CH. Boesch, R. Gruetter, E. Martin, Temporal and spatial analysis of fields generated by eddy currents in superconducting magnets: optimization of corrections and quantitative characterization of magnet/gradient systems, Magn. Reson. Med. 20 (1991) 268–284.

[10] R.E. Wysong, D.P. Madio, I.J. Lowe, A novel eddy current compensation scheme for pulsed gradient systems, Magn. Reson. Med. 31 (1994) 572–575.

[11] H.M. Gach, I.J. Lowe, D.P. Madio, A. Caprihan, S.A. Altobelli, D.O. Kuethe, E. Fukushima, A programmable pre-emphasis system, Magn. Reson. Med. 40 (1998) 427–431.

[12] V.J. Schmithorst, B.J. Dardzinski, Automatic gradient preemphasis: a 15 min journey to improved diffusion-weighted echo planar imaging, Magn. Reson. Med. 47 (2002) 208–212.

[13] H.K. Lee, G.C. Kashmar, O. Nalcioglu, in: Proceedings of ISMRM, Fourth Scientific Meeting and Exhibition, New York, 1996, p. 1406.

[14] M.T. Alley, G.H. Glover, N.J. Pelc, Gradient characterization using a Fourier-transform technique, Magn. Reson. Med. 39 (1998) 581–587.

[15] B.J. Balcom, R.P. MacGregor, S.D. Beyea, D.P. Green, R.L. Armstrong, T.W. Bremner, Single-point ramped imaging with T_1 enhancement (SPRITE), J. Magn. Reson. 123 (1996) 131–134.

[16] G.F. Mason, T. Harshbarger, H.P. Hetherington, Y. Zhang, G.M. Pohost, D.B. Twieg, A method to measure arbitrary **k**-space trajectories for rapid MR imaging, Magn. Reson. Med. 38 (1997) 492–496.